Video Article

Whole Cell Patch Clamp for Investigating the Mechanisms of Infrared Neural Stimulation

William G. A. Brown[1], Karina Needham[2], Bryony A. Nayagam[2], Paul R. Stoddart[1]

[1]Biotactical Engineering, Faculty of Engineering and Industrial Science, Swinburne University of Technology

[2]Department of Otolaryngology, The University of Melbourne

Correspondence to: Paul R. Stoddart at pstoddart@swin.edu.au

URL: https://www.jove.com/video/50444
DOI: doi:10.3791/50444

Keywords: Neuroscience, Issue 77, Biomedical Engineering, Neurobiology, Molecular Biology, Cellular Biology, Physiology, Primary Cell Culture, Biophysics, Electrophysiology, fiber optics, infrared neural stimulation, patch clamp, *in vitro* models, spiral ganglion neurons, neurons, patch clamp recordings, cell culture

Date Published: 7/31/2013

Citation: Brown, W.G., Needham, K., Nayagam, B.A., Stoddart, P.R. Whole Cell Patch Clamp for Investigating the Mechanisms of Infrared Neural Stimulation. *J. Vis. Exp.* (77), e50444, doi:10.3791/50444 (2013).

Abstract

It has been demonstrated in recent years that pulsed, infrared laser light can be used to elicit electrical responses in neural tissue, independent of any further modification of the target tissue. Infrared neural stimulation has been reported in a variety of peripheral and sensory neural tissue *in vivo*, with particular interest shown in stimulation of neurons in the auditory nerve. However, while INS has been shown to work in these settings, the mechanism (or mechanisms) by which infrared light causes neural excitation is currently not well understood. The protocol presented here describes a whole cell patch clamp method designed to facilitate the investigation of infrared neural stimulation in cultured primary auditory neurons. By thoroughly characterizing the response of these cells to infrared laser illumination *in vitro* under controlled conditions, it may be possible to gain an improved understanding of the fundamental physical and biochemical processes underlying infrared neural stimulation.

Video Link

The video component of this article can be found at https://www.jove.com/video/50444/

Introduction

The fields of neurophysiology and medical bionics rely heavily on techniques that allow controllable stimulation of electrical responses in neural tissue. While electrical stimulation remains the gold standard in neural excitation, it suffers from a number of drawbacks such as the presence of stimulation artifacts when recording neural responses, and a lack of stimulation specificity due to the spread of current into surrounding tissue [1].

The last two decades have seen the development of optically mediated stimulation techniques [2]. Several of these techniques require modification of the target tissue, either via the addition of a particular molecule (*e.g.* caged molecules) [3] or some form of genetic manipulation (*e.g.* optogenetics) [4], neither of which are easy to apply outside of a research setting. Of particular interest therefore is infrared neural stimulation (INS), whereby neural tissue is excited by pulsed infrared laser light. INS has the potential to overcome many of the shortcomings of electrical stimulation by enabling highly specific, non-contact stimulation of neural tissue [2]. However, while INS has been successfully demonstrated in a variety of settings *in vivo*, the precise mechanism of excitation remains uncertain.

Some recent publications have shown progress towards uncovering the mechanism behind INS [5-7]. Rapid heating due to absorption of the laser light by water appears to play a key role. However, beyond this a consensus is yet to be reached. Shapiro *et al.* [7] propose a highly general mechanism whereby rapid heating causes a perturbation in the distribution of charged particles adjacent to the cell membrane, leading to a change in the capacitance of the cell membrane and subsequent depolarization. In addition, Albert *et al.* [5] assert that laser induced heating activates a specific class of temperature sensitive ion channels (transient receptor potential vanilloid channels), allowing ions to pass through the cell membrane. At this stage it is unclear how these mechanisms combine, or indeed whether there are further factors that are yet to be identified.

Although a small number of publications (references [5,7-9]) have investigated INS *in vitro*, the vast majority of work published in this field has been carried out *in vivo* (*e.g.* references [1,6,10-18]). Infrared stimulation of auditory neurons has been an area of particular interest, owing to the potential applications in cochlear implants [10,14-18]. While *in vivo* experiments are important to verify the effectiveness of the technique in various settings, the increased level of control afforded by *in vitro* studies is expected to lead to a more detailed understanding of the mechanism responsible for INS. This report describes the preparation of cultured spiral ganglion neurons for patch clamp investigations, as these can be used to study fundamental mechanisms while also linking to the large body of existing data from the auditory system.

The patch clamp technique is an excellent tool for investigations of electrophysiological phenomena, providing a means of recording electrical activity in single cells and studying the contribution of the individual underlying currents[19]. When this technique is applied to a stable *in vitro*

preparation of primary neurons, such as cultured spiral ganglion neurons, it offers the opportunity to study in depth the mechanisms by which neural activity is controlled and manipulated.

The protocols specified in this work outline methods for investigating the effect of laser stimulation on the electrical properties of spiral ganglion neurons through patch clamp recordings. The approach is based on a fiber-coupled laser rather than a free-space laser, allowing safer operation as well as easier and more repeatable alignment without the need to modify the standard microscope configuration. On the basis of these protocols, it should be possible to conduct a wide range of experiments in order to more clearly determine the mechanism or mechanisms behind INS.

Protocol

1. Culture of Spiral Ganglion Neurons

1. Sterilize small round (*e.g.* 10 mm diameter) glass coverslips and curved forceps in an autoclave. Transfer the sterilized coverslips into individual wells of a sterile 4-ring 35 mm petri dish or 4-well plate, using the sterilized forceps. Apply 150 µl of poly-L-ornithine (500 µg/ml) and mouse laminin (0.01 mg/ml) to the top surface of the coverslip and place in an incubator (37 °C) for up to 48 hr. Ensure that the coverslips do not float away from the bottom of the well.
2. Prepare 50 ml sterile Neurobasal media (NBM) for each neural culture: 47.5 ml neurobasal A, 0.5 ml N_2 supplement, 1 ml B27 supplement, 0.5 ml L-glutamine, and 0.5 ml penicillin-streptomycin. Note: Supplements can be frozen, stored at -20 °C and added to the media on the day required.
3. Dissociate spiral ganglion neurons from post-natal day 4-7 rat pups as previously described [20,21], using both enzymatic (0.025% trypsin and 0.001% DNase I) and mechanical techniques. Refer to Whitlon *et al.* [22] and Vieira *et al.* [23] for detailed procedures of spiral ganglion neuron culture, or Parker *et al.* [24] for a demonstration of modiolus isolation.
4. Aspirate any remaining poly-L-ornithine/laminin solution from the coverslips and wash briefly with NBM.
5. Add 150-200 µl of the dissociated spiral ganglion neuron suspension to the coverslips and place into an incubator (37 °C, 10% CO_2). Note: up to 20 coverslips can be prepared from an average litter of 8 rat pups.
6. Four hours after plating neurons, aspirate the solution to remove cell debris and replace with 150-200 µl warmed fresh NBM. Note: media may require daily replenishment to avoid dehydration.
7. Return coverslips to the incubator until required for electrophysiological recordings. Note: dissociated spiral ganglion neuron cultures can be used for electrophysiological experiments four hours after dissociation and for up to two days thereafter. Time *in vitro* should be taken into account during analysis of results. Replenish NBM every 24-48 hr.

2. Preparation for Patch Clamp Recordings

1. Prepare solutions
    1. Intracellular (micropipette) solution: 115 mM K-gluconate, 7 mM KCl, 10 mM HEPES, 0.05 mM EGTA, 2 mM Na_2ATP, 2 mM MgATP, 0.5 mM Na_2GTP (adjust to pH 7.3 with KOH; adjust to 295 mOsmol/kg with sucrose). Pass the solution through a sterile filter (0.2 µm) and divide into 200 µl aliquots to be stored at -20 °C until the day of recording.
    2. Extracellular (bath) solution: 137 mM NaCl, 5 mM KCl, 2 mM $CaCl_2$, 1 mM $MgCl_2$, 10 mM HEPES, 10 mM glucose (adjust to pH 7.4 with NaOH; adjust to 300-310 mOsmol/kg with sucrose). This solution is made on the day of recording.

2. Prepare recording micropipettes with a resistance of 2-6 MΩ. We use a CO_2 laser puller (P-2000; Sutter Instruments) and borosilicate glass (1.0 mm outer diameter; 0.58 mm inner diameter; 75 mm length).
3. Prepare the laser. This protocol is intended for use with a fiber-coupled laser, such as the 1,870 nm Infrared Nerve Stimulator from OptoTech P/L. The optical fiber used for light delivery in our experiments is a 200/220 µm core/cladding diameter silica fiber with a numerical aperture of 0.22 and FC-PC connectors at both ends (AFW Technologies MM1-FC2-200/220-5-C-0.22). The patch cords were cut in half to produce two fiber pigtails (*i.e.* connectorized at one end and cleaved at the other). The effects of fiber core diameter and numerical aperture on laser induced temperature changes have been discussed in detail by Thompson *et al.* [25]
    1. Cleave the tip of the light delivery fiber using standard techniques and ensure that the resulting tip is of high quality by observation with an optical microscope (*i.e.* the tip should be perpendicular to the fiber axis and appear flat upon visual inspection). Connect the light delivery fiber to the fiber-coupled output of the stimulation laser using an appropriate through connector (*e.g.* Thorlabs ADAFC2).
    2. Measure the output laser power from the cleaved tip of the light delivery fiber using an appropriate instrument (*e.g.* Coherent FieldMate with LM-3 detector head). It is recommended to check the laser power every time the light delivery fiber is cleaved or a significant adjustment is made to the laser (*e.g.* transportation from one lab to another).
    3. Insert light delivery fiber into a fiber chuck or equivalent device and affix the chuck to the appropriate micropositioner. It is important to be able to accurately determine the angle θ that the optical fiber makes with the coverslip. This angle can be measured by taking a photograph of the experimental arrangement and using image processing software (*e.g.* ImageJ) to obtain the angle. The angle θ (or range of possible angles) is primarily constrained by spatial limitations of the experimental arrangement - in particular the microscope. Typical values of θ in our experiments (based on an upright microscope) are around 36°, however the optimal angle may differ significantly for alternative setups (*e.g.* those using an inverted microscope).
    4. Make connections between the laser and the patch clamp data acquisition system (*e.g.* Digidata 1440A, Molecular Devices) as shown in **Figure 2**. The digital output from the patch clamp data acquisition system should be connected to the laser via an external function generator, making it possible to specify laser pulse parameters independent of the data acquisition system. Alternatively this output can be connected directly to the laser driver (requiring the pulse length and repetition rate to be set by the data acquisition software). In either case, the signal used to trigger the laser should be connected back to an input of the data acquisition system to ensure that the timing and length of the laser pulses can be recorded concurrently with the electrophysiological signal.

3. Patch Clamp Recordings for Investigation of INS

1. Fill the appropriate container of the perfusion system with extracellular solution and adjust the flow rate to provide perfusion of the bath at a rate of 1-2 ml/min. We use a gravity-fed system (aspirator bottle, pinch valve, and PE tubing) with an in-line heater to enable rapid heating of the solution, and a peristaltic pump to remove spent solution by suction.
2. Place a coverslip with cultured cells into the recording chamber (bath) of an upright microscope. Using a high magnification water-immersion objective (*e.g.* 40X) and phase-contrast (*e.g.* differential interference contrast or Dodt gradient contrast), visually locate the spiral ganglion neurons within the culture. A typical spiral ganglion neuron is phase-bright, round and approximately 15 µm in diameter with a prominent nucleus, as shown in **Figure 1a**.
3. Once a neuron has been located, switch to a lower magnification objective (*e.g.* 10X) and locate the target neuron within the visual field.
4. Move the light delivery optical fiber into position using the following procedure (or equivalent):
    1. Use the micropositioner to move the output fiber until the tip is close to the target neuron in both the horizontal and vertical planes. The vertical position of the fiber tip can be verified by moving the objective up and down (scanning the focus).
    2. Switch back to the high magnification objective and position the tip of the optical fiber in its intended position next to the neuron (see **Figure 2** inset). When adjusting the vertical position of the fiber, it is important that the bottom edge of the fiber is resting on (*i.e.* just touching) the coverslip, to minimize uncertainty in the location of the fiber. Optimal alignment in the horizontal plane will depend on the angle θ that the fiber makes with the coverslip and the radius of the fiber *r*. In order to position the fiber so that the center of the target neuron lies along the fiber axis, the horizontal distance between the upper edge of the fiber and the target cell should be
    $\Delta_{target} = r$ (cosec θ - 2 sin θ),
    where negative values would indicate that the optical fiber overhangs the cell. When aligning the fiber, a distance of Δ_{target} between the top edge of the fiber and the center of the neuron can be approximately achieved by visual inspection. However Δ_{target} is designed to serve as a rough guideline only. Positioning the fiber such that the actual distance Δ between the upper edge of the fiber and the center of the neuron differs measurably from Δ_{target} (as in **Figure 1**) can provide insight into the effect of both radial displacement (*i.e.* from the center of the beam) and axial displacement (*i.e.* along the fiber axis) of the beam relative to the target neuron. For example, setting Δ ≈ 0 would be expected to increase the local temperature in the vicinity of the cell - *i.e.* since the beam profile for typical multimode fibers is well approximated by a top hat distribution [26], the decrease in locally absorbed energy (temperature) due to displacement from the center of the beam is minimal compared to the increase in absorbed energy from moving the fiber end face closer to the cell.
    While care should be taken to position the fiber as accurately and repeatably as possible using visual cues, precise measurement of the fiber location relative to the target neuron (*e.g.* Δ) is of greater importance than positioning it a predetermined distance away. Δ can be determined (with an estimated maximum uncertainty of ±3 µm) by image analysis as described in step 3.8.2 of the protocol. In some experiments [5,8], white light sources have been coupled through the fiber in order to target the desired cell. This approach was found to be ineffective in the upright microscope setup, as the intensity of light scattered from the target region was relatively low at these shallow angles (θ).
    3. Once the fiber is in position, move it out by a known amount to enable straightforward positioning of the micropipette. The fiber can then be returned to the original position when a neural recording is achieved.

5. Fill the micropipette with intracellular solution and securely fit into place on the headstage of the amplifier (*e.g.* Multiclamp 700B, Molecular Devices). Using tubing attached to the side of the microelectrode holder, apply a small amount of positive pressure to prevent clogging of the micropipette.
6. Using a micromanipulator, move the micropipette into position just above the target neuron.
7. Protocol for whole cell recordings:
    1. Apply a 10 msec, +10 mV square wave pulse (*e.g.* Seal Test) in voltage-clamp mode of the amplifier and adjust the micropipette potential (pipette offset) of the baseline signal to 0 nA. The seal test should also be used to determine whether the resistance of the microelectrode is within the desired range (*e.g.* 2 - 6 MΩ).
    2. While monitoring the resistance, use fine adjustments of the micromanipulator to gently position the micropipette onto the surface of the target neuron. When the micropipette is in contact with the neuron, the resistance will increase (by ~ 0.5 to 1 MΩ). Immediately following the resistance increase, remove the positive fluid pressure and apply a small negative pressure. Once resistance has passed 10 - 20 MΩ, fix the membrane potential to a holding level (*e.g.* around -60 mV).
    3. The electrode resistance should continue to increase until it exceeds 1 GΩ, signifying that an effective seal (termed 'gigaseal') has been formed between the cell membrane and micropipette. At this point, remove all fluid pressure from the micropipette.
    4. Once the gigaseal has been formed, use short current pulses (25 to 100 µsec; +1 V) or brief pulses of negative fluid pressure to rupture the cell membrane and achieve whole cell configuration.
    5. Record the membrane capacitance, series resistance and input resistance as determined from the exponential curve fitted to the current during the seal test pulse. Minimize the capacitance transients by adjusting the CpFast and CpSlow controls on the amplifier, then switch the amplifier into whole cell mode, and compensate capacitance and resistance until a flat current is observed during the seal test. Apply series resistance compensation (~70% correction; 70% prediction), adjusting capacitance and resistance controls to maintain a flat test seal response.
    6. Switch to current-clamp mode in the amplifier. Take note of the resting membrane potential (in the absence of current injection). Set a holding current to stabilize the membrane potential at the desired level (*e.g.* -60 mV). Neutralize the pipette capacitance and adjust the bridge balance to balance the voltage drop.
    7. Check the firing properties of the neuron by stimulating with depolarizing current (+10 to +200 pA in +10 pA steps; 300 msec duration).

8. 1. Move the optical fiber back into position next to the neuron. Using imaging software coupled to a CCD camera, capture images of the position of the fiber with respect to the target neuron, focusing on the plane of the neuron initially, and then on the top edge of the optical fiber (see **Figure 1**).
    2. By subsequent analysis of the resulting images (*e.g.* **Figures 1b** and **1c**) it is possible to precisely determine Δ (the position of the upper edge of the optical fiber relative to the center of the target neuron). Once Δ is known, parameters such as the distance from the fiber end face to the target neuron (along the fiber axis) *z* and the radial displacement of the neuron from the center of the beam δ*r* can be calculated using simple trigonometric relations:

$z = r \sin 2\theta + \Delta \cos \theta$
$\delta r = ((r \cos 2\theta - \Delta \sin \theta)^2 + \delta y^2)^{1/2}$,
where δy is the distance between the fiber axis and the center of the neuron as seen from above (*e.g.* see **Figure 1**).
Analysis should take into account positional variations from cell to cell, as accurate knowledge of these location parameters may be required to resolve possible differences between stimulation processes [25].

4. INS Experiments

1. While recording electrophysiological data in either current clamp or voltage clamp configurations, run the stimulation laser at the desired parameters (*e.g.* power, pulse length, repetition rate etc.). With our laser, the optical power is controlled via a direct input to the laser driver and is specified manually before each recording. Pulse length and repetition rate can be controlled by either an external signal generator or the data acquisition software (as described in step 2.3.4). Ensure that data are recorded from both the patch clamp channel and the laser trigger channel.

Laser pulses with lengths ranging from around 500 µsec to 15 msec and energies of ~0.25-5 mJ per pulse typically yield measurable electrical responses. Setting the repetition rate of laser pulses to be 1 Hz or less may be useful for initial experiments, since it will minimize the effects of this parameter. Typical results showing the change in the recorded signal are presented in the following Section.

Representative Results

Spiral ganglion neurons respond to laser illumination with repeatable waveforms in both voltage-clamp and current-clamp recording configurations. **Figure 3a** shows typical changes in current flow across a cell membrane in response to a 2.5 msec, 0.8 mJ laser pulse (average response from 6 laser pulses, repeated at 1 sec intervals) with the membrane potential held at -70 mV, -60 mV and -50 mV. Net inward currents are consistently evoked in response to laser pulses, returning to initial values after illumination has ceased. The shape of the laser induced currents can be seen to vary as the membrane potential is changed, indicating that it may be important to conduct experiments at a range of holding potentials in order to gain a complete understanding of the processes underlying INS. These experiments can be carried out with minor modification of the current protocol and analyzed using established techniques such as charge-voltage (Q-V) analysis (see Reference [7] for examples of Q-V curves obtained from INS *in vitro*).

The data presented in **Figure 3b** are indicative of the change in membrane potential typically evoked by a 2.5 msec, 0.8 mJ laser pulse (initial membrane potential -73mV, averaged over 16 laser pulses delivered at a repetition rate of 4 Hz). Current-clamp recordings show a steady membrane depolarization over the course of the laser pulse followed by an approximately exponential decrease towards the resting membrane potential after the pulse. The example in **Figure 3b** also exhibits a small additional membrane depolarization following the laser pulse. Shapiro *et al.* [7] have demonstrated that laser-induced changes in membrane potential are closely related to local changes in temperature (*i.e.* the temperature in the direct vicinity of the cell). Further, the model described by Thompson *et al.* [27] has determined that under certain alignment conditions, diffusion resulting from axial and radial temperature gradients in the illuminated region can lead to local temperature variations closely resembling the changes in membrane potential shown in **Figure 3b**. As a result of these findings, it is thought that the position of the target cell relative to the end-face of the light delivery fiber plays a significant role in determining both the time course of laser-evoked variations in membrane potential and the maximum temperature in the region of the cell.

Illuminating with excessive energy or exposure to large increases in temperature may result in damage to the target neuron. This can often be observed through deterioration of cell electrical properties (*e.g.* an abrupt increase in current required to maintain the membrane potential at a steady level, and/or a large increase in noise and instability within the signal). In extreme cases cell death occurs almost instantaneously upon laser exposure. **Figure 4** shows a voltage-clamp recording of the death of a spiral ganglion neuron resulting from exposure to a 25 msec, 8 mJ laser pulse.

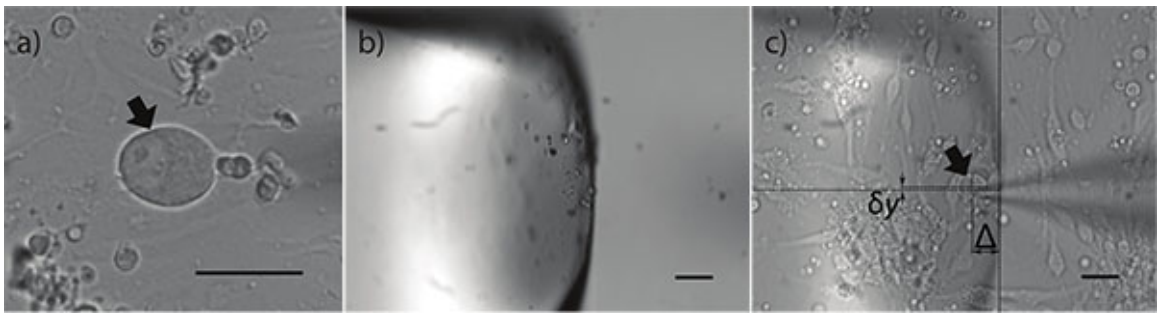

Figure 1. Phase contrast images showing a typical spiral ganglion neuron and the relative positions of optical fiber and micropipette (as seen from above) during optical stimulation experiments. a) Typical spiral ganglion neuron. **b)** The optical fiber in position (image is focused on the top edge of the optical fiber). **c)** Overlaid images showing the fiber position relative to the cell (note: the top edge of the fiber is slightly overhanging the cell *i.e.* Δ is negative). As seen from above, δ*y* and Δ are the radial displacement of the neuron center from the fiber axis and the distance from the top edge of the fiber to the center of the neuron respectively. Arrows indicate the position of the spiral ganglion neuron. Scale bars 20 µm.

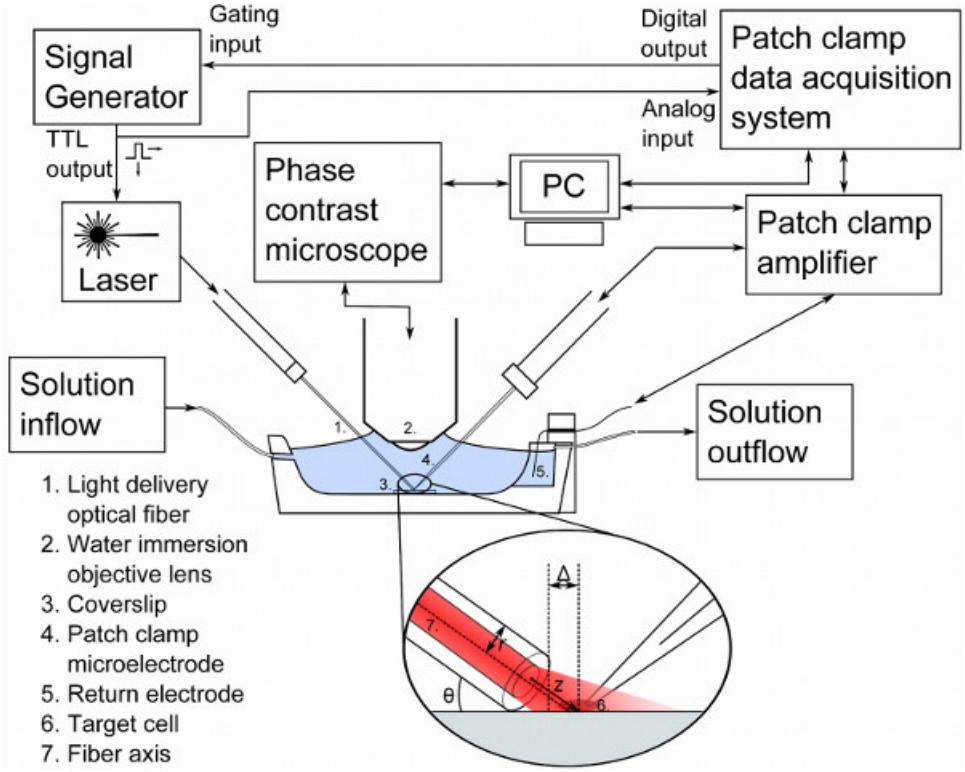

Figure 2. Schematic of the experimental setup for optical stimulation experiments (not to scale). Inset: position of optical fiber and microelectrode relative to the target cell. θ, Δ and *z* are as defined in protocol steps 3.4.2 and 3.8.2.

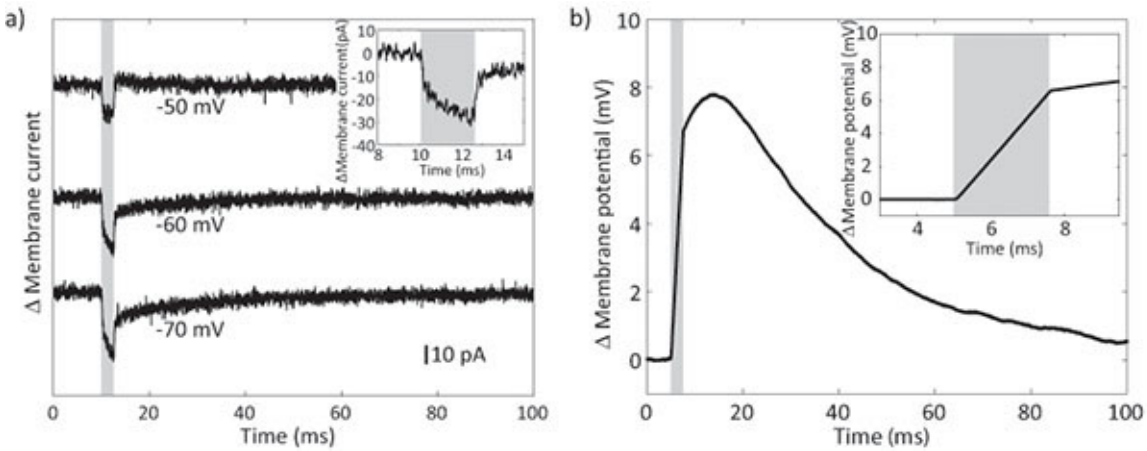

Figure 3. a) Voltage-clamp (average response from 6 laser pulses delivered at a rate of 1 Hz) and **b)** current-clamp (average response from 16 laser pulses repeated at a rate of 4 Hz) recordings from spiral ganglion neurons showing laser induced changes in membrane current and membrane potential upon illumination by a 2.5 msec, 0.8 mJ laser pulse. Shaded regions indicate the timing of laser exposure. Insets show responses during laser illumination in more detail. Note: the inset in **a)** focuses on the trace obtained with a membrane potential of -60 mV. Click here to view larger figure.

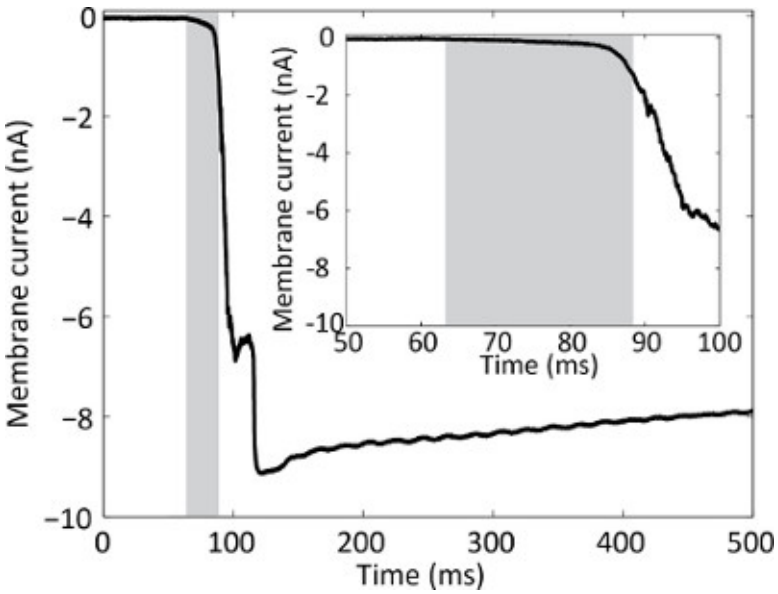

Figure 4. Voltage-clamp recording showing cell death resulting from exposure to an excessively energetic (25 msec, 8 mJ) laser pulse. Note that the amplitude of the signal is shown in nA and is significantly larger than the pA currents shown in **Figure 3**.

Discussion

Using the protocols outlined in this paper it is possible to extract and culture spiral ganglion neurons and to investigate laser-evoked electrical activity by performing whole cell patch clamp experiments. When used *in vitro*, the patch clamp technique provides a level of control over experimental parameters that is not achievable *in vivo*. Laser stimulation parameters such as wavelength, pulse energy, pulse length, pulse shape, and pulse repetition sequences can be studied in a reproducible setting. In addition, the environment in which the neurons are maintained (*e.g.* solution temperature, chemical factors) can be systematically varied, making it possible to study the membrane properties and hence the mechanisms underlying infrared neural stimulation. The interaction between electrical and optical stimulation modalities can also be investigated in a controlled manner. These fundamental studies can be further advanced by introducing fluorescent probes to monitor additional parameters such as ionic concentrations or the expression of heat shock proteins. A clear understanding of these various parameters is not only critical to achieve a complete understanding of the phenomenon, but also to achieve more efficient stimulation through process optimization.

Due to the important role played by temperature in the mechanism of INS [5-7], accurate measurement of the localized heating due to laser illumination is of paramount importance in defining this mechanism [27]. A detailed method of obtaining calibrated temperature measurements by recording the current flowing through an open patch pipette has been described by Yao *et al.* [28] and employed by numerous authors, to determine the magnitude and time course of laser induced temperature changes in environments representative of those found *in vitro* (*e.g.* see References [7, 8]). Provided the position of the light delivery fiber can be precisely determined (*e.g.* using the current protocol), this method of temperature measurement is likely to enable accurate mapping of the local change in temperature due to typical INS stimuli.

The wavelength of the stimulating laser is a parameter that should be considered in INS experiments, since laser induced temperature changes (and hence the underlying mechanisms of INS) are mediated by the wavelength dependent absorption characteristics of water [7] (see Thompson *et al.* [25] for a detailed discussion of expected wavelength effects). Aside from the 1,870 nm diode laser used in this protocol (Infrared Nerve Stimulator, Optotech P/L), a variety of wavelengths and laser packages have been used by other authors. Some common examples of the lasers used in existing INS publications are: diode lasers from Aculight with wavelengths ranging from 1,840-1,940 nm [6,7,10,13,16-18]; Holmium:YAG lasers (2.12 µm) from Laser 1-2-3 [6,11,12,14,15]; and diode lasers operating at 1,875 nm[5,8], 1,470 nm [8], and 1,535 nm [8] from Sheaumann laser.

A potential drawback of applying this technique to cultured spiral ganglion neurons is that owing to the relatively small size of the neurons (~10-15 µm diameter), the recording electrode is directly illuminated by the laser. It has been suggested that laser illumination beyond a certain threshold may change the properties of the recording circuit [7] (*i.e.* seal and pipette resistance). Shapiro *et al.* [7] measured this threshold by monitoring the change in reversal potential of Q-V curves as laser power was increased, finding a threshold pulse energy of 3 mJ. As an alternative approach, it may be possible to determine the magnitude of this effect by measuring the combined resistance of the seal and pipette in whole cell mode (*e.g.* by recording the current response to a 10 msec, +10 mV voltage pulse) while varying the temperature of the extracellular solution. In order to fully understand the mechanisms of INS, it is vital that laser induced resistance changes be measured and taken into account.

To date the majority of experimental work concerning infrared neural stimulation has been undertaken *in vivo*. While reported radiant exposure thresholds for infrared stimulation *in vivo* vary somewhat (*e.g.* 0.32 Jcm^{-2} at 2.12 µm for rat sciatic nerves [1], <0.1 Jcm^{-2} at 1.855 µm for gerbil auditory nerves [18]), they are significantly lower than thresholds determined through *in vitro* studies (*e.g.* approximately 20 Jcm^{-2} at 1.875 µm for mouse retinal ganglion cells and rat vestibular ganglion cells [5,8], 8.3 J cm^{-2} for rat neonatal cardiomycytes [9]). At this stage the details of the INS process are not sufficiently well understood to speculate about the cause of this difference; however, using *in vitro* models such as auditory neurons that closely resemble the targets of previous *in vivo* work may be advantageous in finding an explanation.

Some other *in vitro* models involve larger cells such as *Xenopus* oocytes (~1 mm diameter) used by Shapiro *et al.* [7] These may be useful for probing spatial variations in the effectiveness of INS across individual cells in order to investigate whether cellular components are influenced

by stimulation. Simpler models such as lipid bilayer vesicles may allow even more precise control over experimental parameters than *in vitro* experiments, however such models are somewhat limited in scope and may not reveal the full complexity of INS.

Disclosures

The authors have nothing to disclose.

Acknowledgements

This work was supported by the Australian Research Council under Linkage Project grant LP120100264.

References

1. Wells, J., Kao, C., Jansen, E.D., Konrad, P., & Mahadevan-Jansen, A. Application of infrared light for *in vivo* neural stimulation. *Journal of Biomedical Optics.* **10**, 064003, doi:10.1117/1.2121772 (2005).
2. Richter, C.P., Matic, A.I., Wells, J.D., Jansen, E.D., & Walsh, J.T. Neural stimulation with optical radiation. *Laser & Photonics Reviews.* **5**, 68-80, doi:10.1002/lpor.200900044 (2011).
3. Kramer, R.H., Fortin, D.L., & Trauner, D. New photochemical tools for controlling neuronal activity. *Current Opinion in Neurobiology.* **19**, 544-552 (2009).
4. Boyden, E.S., Zhang, F., Bamberg, E., Nagel, G., & Deisseroth, K. Millisecond-timescale, genetically targeted optical control of neural activity. *Nature Neuroscience.* **8**, 1263-1268, doi:10.1038/nn1525 (2005).
5. Albert, E.S., *et al.* Trpv4 channels mediate the infrared laser-evoked response in sensory neurons. *Journal of Neurophysiology.* **107**, 3227-3234 (2012).
6. Wells, J., *et al.* Biophysical mechanisms of transient optical stimulation of peripheral nerve. *Biophysical Journal.* **93**, 2567-2580, doi:10.1529/biophysj.107.104786 (2007).
7. Shapiro, M.G., Homma, K., Villarreal, S., Richter, C.-P., & Bezanilla, F. Infrared light excites cells by changing their electrical capacitance. *Nature Communications.* **3**, 736, doi:10.1038/ncomms1742 (2012).
8. Bec, J.-M., *et al.* Characteristics of laser stimulation by near infrared pulses of retinal and vestibular primary neurons. *Lasers in Surgery and Medicine.* **44**, 736-745, doi:10.1002/lsm.22078 (2012).
9. Dittami, G.M., Rajguru, S.M., Lasher, R.A., Hitchcock, R.W., & Rabbitt, R.D. Intracellular calcium transients evoked by pulsed infrared radiation in neonatal cardiomyocytes. *Journal of Physiology (London).* **589**, 1295-1306, doi:10.1113/jphysiol.2010.198804 (2011).
10. Izzo, A.D., *et al.* Laser stimulation of auditory neurons: Effect of shorter pulse duration and penetration depth. *Biophysical Journal.* **94**, 3159-3166, doi:10.1529/biophysj.107.117150 (2008).
11. Wells, J., Konrad, P., Kao, C., Jansen, E.D., & Mahadevan-Jansen, A. Pulsed laser versus electrical energy for peripheral nerve stimulation. *Journal of Neuroscience Methods.* **163**, 326-337, doi:10.1016/j.jneumeth.2007.03.016 (2007).
12. Teudt, I.U., Nevel, A.E., Izzo, A.D., Walsh, J.T., & Richter, C.P. Optical stimulation of the facial nerve: A new monitoring technique? *Laryngoscope.* **117**, 1641-1647, doi:10.1097/M1LG.0b013e318074ec00 (2007).
13. Jenkins, M.W., *et al.* Optical pacing of the embryonic heart. *Nature Photonics.* **4**, 623-626, doi:10.1038/nphoton.2010.166 (2010).
14. Izzo, A.D., Richter, C.P., Jansen, E.D., & Walsh, J.T. Laser stimulation of the auditory nerve. *Lasers in Surgery and Medicine.* **38**, 745-753, doi:10.1002/lsm.20358 (2006).
15. Izzo, A.D., *et al.* Selectivity of neural stimulation in the auditory system: A comparison of optic and electric stimuli. *J. Biomed. Opt.* **12**, 021008 (2007).
16. Richter, C.P., *et al.* Optical stimulation of auditory neurons: Effects of acute and chronic deafening. *Hearing Research.* **242**, 42-51, doi:10.1016/j.heares.2008.01.01 (2008).
17. Littlefield, P.D., Vujanovic, I., Mundi, J., Matic, A.I. & Richter, C.P. Laser stimulation of single auditory nerve fibers. *Laryngoscope.* **120**, 2071-2082, doi:10.1002/lary.21102 (2010).
18. Izzo, A.D., *et al.* Optical parameter variability in laser nerve stimulation: A study of pulse duration, repetition rate, and wavelength. *IEEE Transactions on Biomedical Engineering.* **54**, 1108-1114, doi:10.1109/tbme.2007.892925 (2007).
19. Sakmann, B. & Neher, E. Patch clamp techniques for studying ionic channels in excitable-membranes. *Annual Review of Physiology.* **46**, 455-472, doi:10.1146/annurev.physiol.46.1.455 (1984).
20. Needham, K., Nayagam, B.A., Minter, R.L., & O'Leary, S.J. Combined application of brain-derived neurotrophic factor and neurotrophin-3 and its impact on spiral ganglion neuron firing properties and hyperpolarization-activated currents. *Hearing Research.* **291**, 1-14 (2012).
21. Coleman, B., Fallon, J.B., Pettingill, L.N., de Silva, M.G., & Shepherd, R.K. Auditory hair cell explant co-cultures promote the differentiation of stem cells into bipolar neurons. *Experimental Cell Research.* **313**, 232-243, doi:10.1016/j.yexcr.2006.10.010 (2007).
22. Whitlon, D.S., *et al.* Survival and morphology of auditory neurons in dissociated cultures of newborn mouse spiral ganglion. *Neuroscience.* **138**, 653-662, doi:10.1016/j.neuroscience.2005.11.030 (2006).
23. Vieira, M., Christensen, B.L., Wheeler, B.C., Feng, A.S., & Kollmar, R. Survival and stimulation of neurite outgrowth in a serum-free culture of spiral ganglion neurons from adult mice. *Hearing Research.* **230**, 17-23, doi:10.1016/j.heares.2007.03.005 (2007).
24. Parker, M., Brugeaud, A., & Edge, A.S.B. Primary culture and plasmid electroporation of the murine organ of corti. *J. Vis. Exp.* (36), doi:10.3791/1685 (2010).
25. Thompson, A.C., Wade, S.A., Brown, W.G.A., & Stoddart, P.R. Modeling of light absorption in tissue during infrared neural stimulation. *Journal of Biomedical Optics.* **17**, 075002 (2012).
26. Snyder, A.W. & Love, J.D. *Optical Waveguide Theory.*, Chapman and Hall, (1983).
27. Thompson, A.C., Wade, S.A., Cadusch, P.J., Brown, W.G.A., & Stoddart, P.R. Modelling of the temporal effects of heating during infrared neural stimulation. *J. Biomed. Opt.* **18**, 035004, doi:10.1117/1.JBO.18.3.035004 (2013).

28. Yao, J., Liu, B.Y., & Qin, F. Rapid temperature jump by infrared diode laser irradiation for patch-clamp studies. *Biophysical Journal.* **96**, 3611-3619, doi:10.1016/j.bpj.2009.02.016 (2009).

